

# Structural and Physical Properties of Silk Fibroin/Alginate Blend Sponges

Kwang-Gill Lee,<sup>1</sup> HaeYong Kweon,<sup>1</sup> Joo-Hong Yeo,<sup>1</sup> Soon-Ok Woo,<sup>1</sup> Jang-Hern Lee,<sup>2</sup> Young Hwan Park<sup>3</sup>

<sup>1</sup>Department of Sericulture and Entomology, National Institute of Agricultural Science and Technology, Suwon 441-100, Korea

<sup>2</sup>College of Veterinary Medicine, Seoul National University, Suwon 441-744, Korea

<sup>3</sup>School of Biological Resources and Materials Engineering, Seoul National University, Suwon 441-744, Korea

Received 11 August 2003; accepted 27 February 2004

DOI 10.1002/app.20714

Published online in Wiley InterScience (www.interscience.wiley.com).

**ABSTRACT:** Silk fibroin/alginate blend sponges were examined through IR spectroscopy, X-ray diffractometry, and differential scanning calorimetry to determine the structural changes of silk fibroin. The effects of fibroin/alginate blend ratios on the physical and mechanical properties were investigated to discover the feasibility of using these blend sponges as biomedical materials such as wound dressings. The compressive modulus of silk fibroin was increased up to 30 kPa, from 7.1 kPa, by blending with alginate. Thermal

crystallization behavior of fibroin induced by heat treatment was restricted by blending with alginate. In spite of that, the structural characteristics of fibroin were not changed by incorporation with alginate. © 2004 Wiley Periodicals, Inc. *J Appl Polym Sci* 93: 2174–2179, 2004

**Key words:** silk fibroin; alginate; conformational analysis; mechanical properties; blends

## INTRODUCTION

Silk fibroin (SF) is a typical protein polymer produced by the silkworm, *Bombyx mori*. SF has been used as a textile fiber and surgical suture for thousands of years because of its unique gloss, handle, and mechanical properties. Recently, SF has been intensively studied with respect to diverse usage for biotechnological and biomedical fields because of its reproducibility, environmental compatibility, nontoxicity, and biological compatibility. Based on its biocompatibility, the possible uses of regenerated SF have been proposed, including substrate for cell culture,<sup>1,2</sup> enzyme immobilization,<sup>3,4</sup> and matrix for drug release.<sup>5</sup> However, the collective properties, especially mechanical properties of SF sponges in the dry state, are too weak to handle SF as wound dressing.

To improve its collective properties, blending with other polymers is useful. The polymer blend technique has been used for many years. Some researchers reported the physical properties of SF films can be enhanced by blending it with other synthetic or natu-

ral polymers, such as poly(vinyl alcohol),<sup>6</sup> chitosan,<sup>7</sup> and sodium alginate,<sup>8</sup> for example.

Sodium alginate (SA), obtained from brown seaweeds, is a linear 1,4-linked copolymer of  $\beta$ -D-mannuronic acid and  $\alpha$ -L-guluronic acid residues. A typical polysaccharide, SA is known to be nontoxic biocompatible polymer. Recently, SA has been investigated in such uses as matrix for drug delivery,<sup>9,10</sup> scaffold for specific cell culture,<sup>11</sup> and wound dressing,<sup>12</sup> for example.

The objective of the present work was to study the structural characteristics and mechanical properties of SF/SA blend sponges. The molecular conformation and crystalline structure of SF/SA blend sponges were investigated through infrared spectroscopy, X-ray diffractometry, and differential scanning calorimetry. Mechanical properties of SF/SA blend sponges were measured by mechanical tester.

## EXPERIMENTAL

### Materials

Raw silk was degummed twice with 0.5% on the weight of fiber (o.w.f.) marseilles soap and 0.3% o.w.f. sodium carbonate solution at 100°C for 1 h and then washed with distilled water. Degummed silk was dissolved in  $\text{CaCl}_2 : \text{H}_2\text{O} : \text{ethanol} = 1 : 8 : 2$  in volume. The fibroin solution was obtained after dialysis of dissolved fibroin solution against distilled water for 4 days, and then stored in refrigerator before use.

Correspondence to: H.-Y. Kweon (hykweon@rda.go.kr).

Contract grant sponsor: Korea Science and Engineering Foundation (KOSEF); contract grant number: R01-2002-000-00391-0

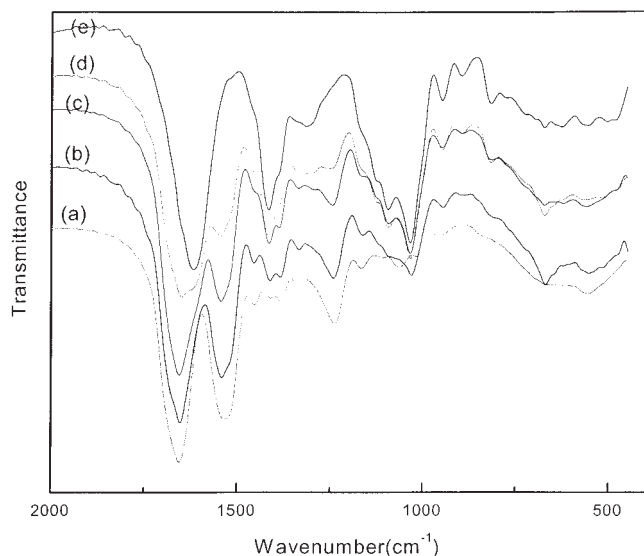


**Figure 1** FTIR spectra of fibroin/alginate blend sponges: (a) 10 : 0; (b) 7 : 3; (c) 5 : 5; (d) 3 : 7; and (e) 0 : 10.

Sodium alginate (SA) was purchased from Wako Pure Chemicals (Tokyo, Japan) and dissolved in distilled water at 50°C for 3 h to prepare a 1 wt % solution.

#### Preparation of blend film

The casting solutions of SF/alginate blend sponges were prepared by mixing the aqueous SF and alginate solutions. Each solution was mixed with weight ratios of SF to SA to be 10 : 0, 7 : 3, 5 : 5, 3 : 7, and 0 : 10 and stirred at room temperature for 30 min. The mixed solution was cast onto polystyrene dishes and lyophilized to obtain blend sponges.

#### Measurements

FTIR spectra were obtained using a Paragon 1000 FTIR spectrometer (Perkin Elmer Cetus Instruments, Norwalk, CT) in the spectral region of 1400–500  $\text{cm}^{-1}$ .

The X-ray diffraction (XRD) analysis were performed with small-angle X-ray scattering with a general area detector diffraction system (GADDS, Bruker AXS, Karlsruhe, Germany), using  $\text{Cu-K}\alpha$  radiation with a wavelength of 1.5418 Å, under irradiation conditions of 40 kV and 30 mA.

DSC curves were obtained by use of a TA 2910 instrument (TA Instruments, New Castle, DE) at a heating rate of 10°C/min and nitrogen gas flow rate of 50 mL/min. The samples were heated first to 150°C and then annealed at 150°C in a DSC sample pan for 10 min. Second heating scans were run to 400°C after quenching from 150°C to room temperature.

The mechanical properties of the SF/alginate sponges were examined by use of a Minimat (Rheo-

metric Scientific, Piscataway, NJ), using  $5 \times 5 \times 0.5$  mm samples, at a crosshead rate of 1 mm/min. The compressive modulus was calculated as the slope of the initial linear portion of the stress–strain curve. DSC curves were obtained with a thermal analysis instrument (TA 2910) at a heating rate of 10°C/min and a nitrogen gas flow rate of 50 mL/min.

Morphology of SF/alginate blend sponges was observed through a scanning electron microscope (LEO1250; LEO Electron Microscopy, now The Nano Technology Systems Division of Carl Zeiss NTS GmbH, Oberkochen, Germany) after gold and palladium coating.

## RESULTS AND DISCUSSION

#### FTIR spectra

Many researchers often investigate the conformation of SF and its blend using FTIR spectroscopy because the IR spectrum represents typical absorption bands sensitive to the molecular conformation of SF. The IR spectra of SF/alginate blend sponges with different compositions are shown in Figure 1. SF sponges [Fig. 1(a)] showed strong absorption bands at 1651 (amide I), 1531 (amide II), and 1236  $\text{cm}^{-1}$  (amide IV), which were attributed to random coil conformation of SF.<sup>7,13</sup>

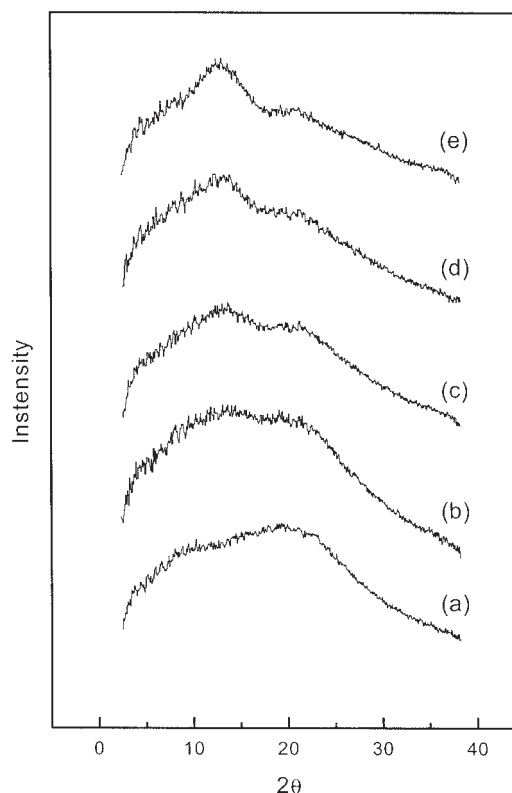


**Figure 2** X-ray diffraction patterns of fibroin/alginate blend sponges: (a) 10 : 0; (b) 7 : 3; (c) 5 : 5; (d) 3 : 7; and (e) 0 : 10.

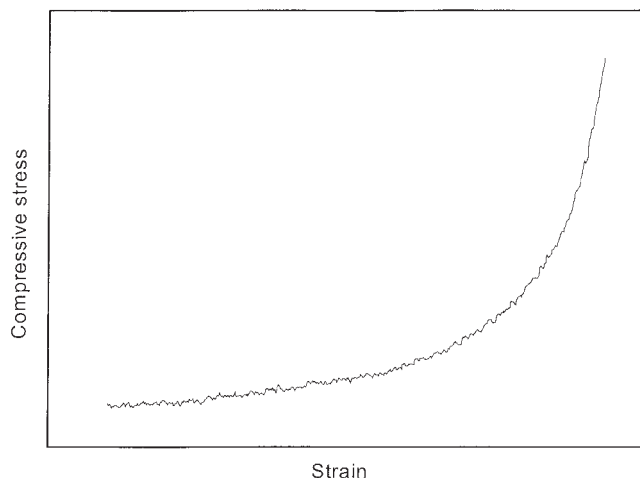


**Figure 3** Compressive stress–strain curves of fibroin/alginate blend sponges.

The hydrogen-bonded amide II band at around  $1520\text{ cm}^{-1}$  is also shown in SF sponges and decreased with an increase of SA. On the other hand, SA [Fig. 1(e)] showed strong absorption bands at  $1620$  ( $-\text{COO}-$  asymmetric stretching),  $1418$  ( $-\text{COO}-$  symmetric stretching), and  $1050\text{ cm}^{-1}$  (CN stretching).<sup>14,15</sup> The characteristic peaks of SF and SA in SF/SA blend sponges were not changed with blending ratios of the two polymers because either the two polymers did not mutually interact or their interaction was too weak to detect by FTIR spectroscopy.

### X-ray diffractometry

The X-ray diffraction patterns of blend sponges reflect that the crystalline structure of these sponges. Therefore, to examine the effect of blending ratio on the

crystalline structure of SF blend sponges, X-ray diffraction patterns of the SF/SA blend sponges were observed (Fig. 2). SA showed a diffraction peak at  $2\theta = 13.4^\circ$ . The X-ray diffraction patterns of the blend sponges vary with their compositions. These results indicated that each material did not affect the crystalline structure of another material.

### Mechanical properties

The representative compressive stress–strain curves of the SF/alginate blend sponges are shown in Figure 3. The deformation of SF/SA sponges occurred through three distinct region: a linear-elastic region, followed by a plateau of roughly constant stress, leading into a final region of steeply increasing stress. The compressive modulus of SF and SF blend sponges was calculated from the stress–strain curves (Fig. 4). The compressive moduli of SF itself and alginate sponge were  $7.1$  and  $45.9\text{ kPa}$ , respectively. Regardless of the blend ratio, that of SF/alginate blend sponges showed around  $30\text{ kPa}$ , which was much higher than that of SF itself. The results indicate that the mechanical properties of SF/alginate blend sponge was dependent on the existence of alginate, given that alginate is composed of a rigid polysaccharide chain.

According to the tensile properties data of SF blend films contributed by many researchers,<sup>7,8,16,17</sup> similar results were reported for the breaking strength of SF/polysaccharide blend films (including chitosan, cellulose, alginate, and polyglutamate), which was generally increased with increasing polysaccharide content. Considering the mechanical properties of silk fibroin blend films and sponges, it can be concluded that polysaccharides are useful additives for improvement of mechanical properties of silk fibroin-based materials.

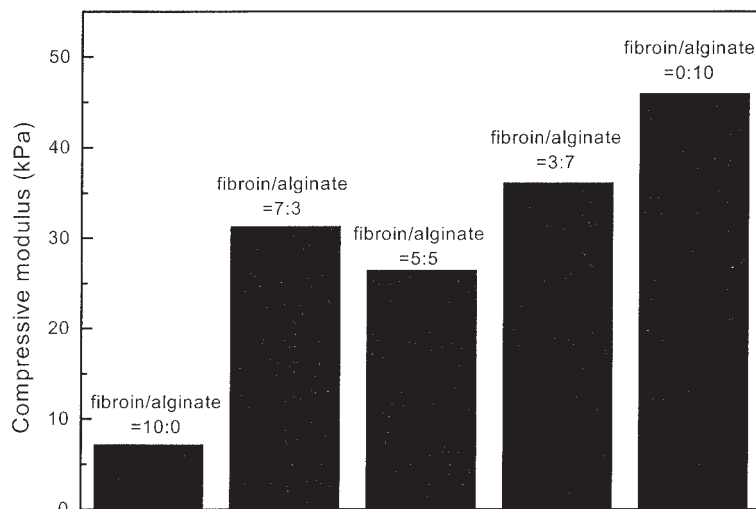


**Figure 4** Compressive mechanical modulus of fibroin/alginate blend sponges.

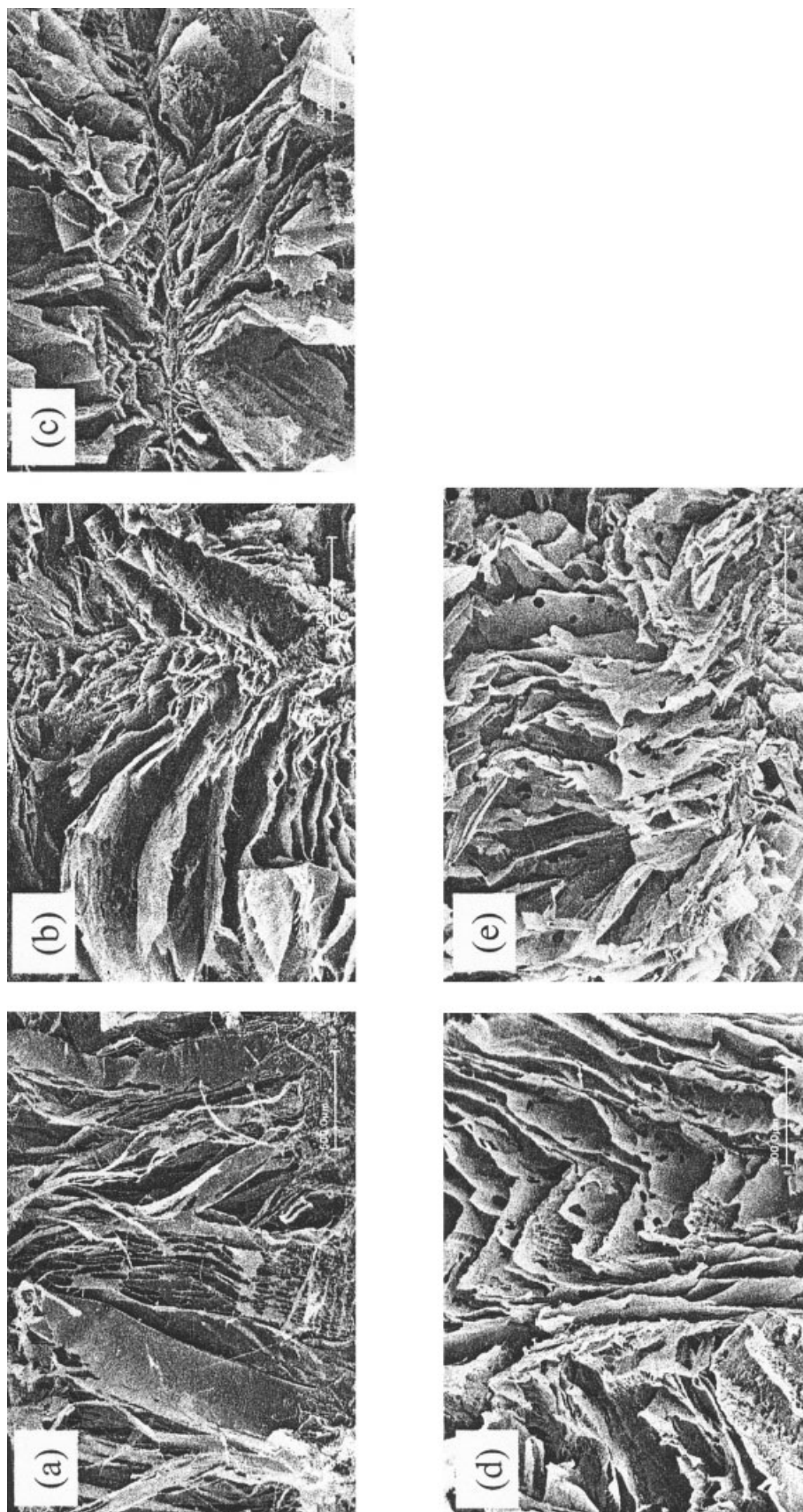


Figure 5 SEM microphotographs of fibroin/alginate blend sponges: (a) 10 : 0; (b) 7 : 3; (c) 5 : 5; (d) 3 : 7; and (e) 0 : 10.

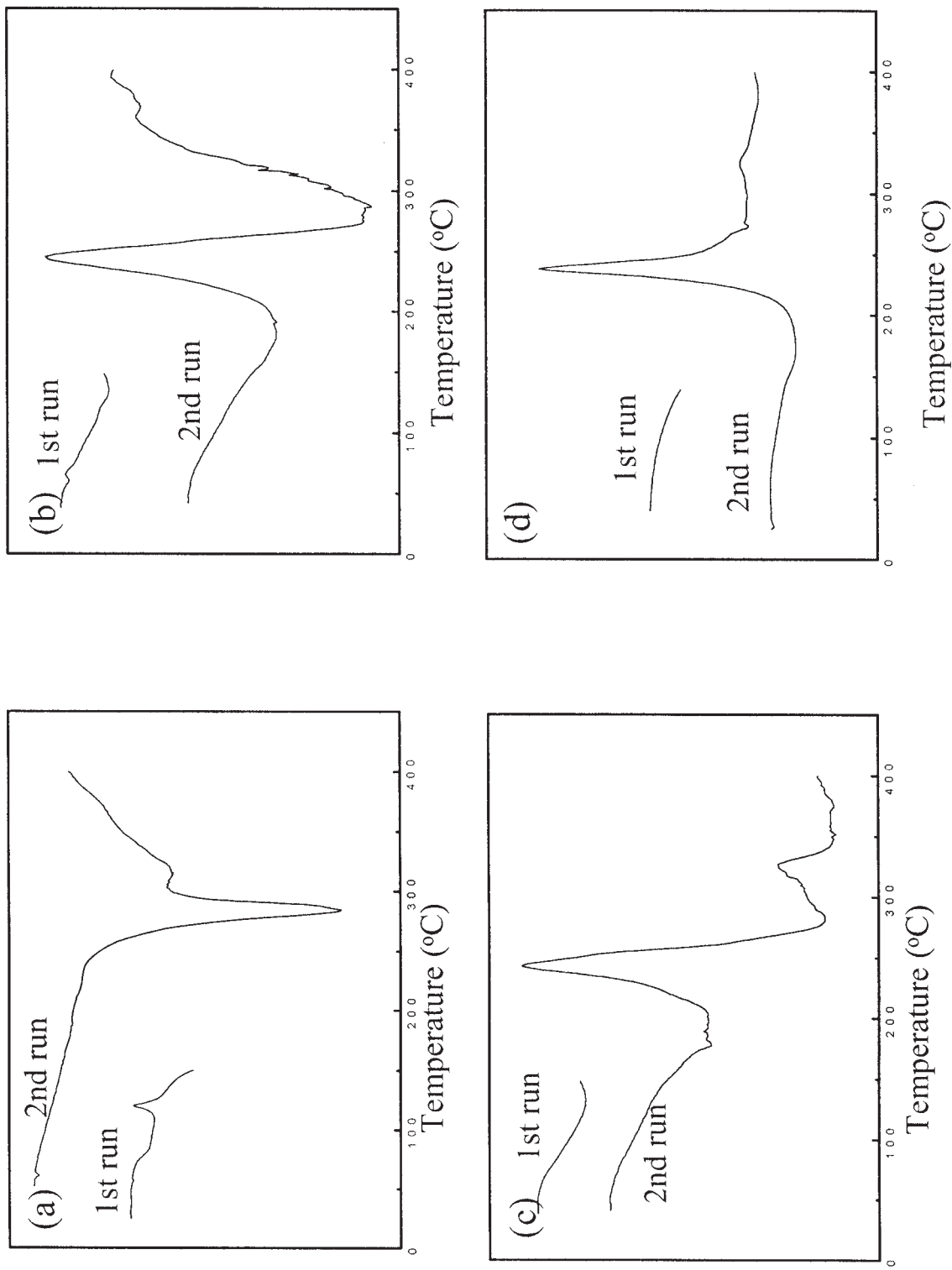


Figure 6 DSC thermograms of fibroin/alginate blend sponges: (a) 10 : 0; (b) 7 : 3; (c) 5 : 5; and (d) 0 : 10.

### Scanning electron microscopy

SEM microphotographs of SF/alginate blend sponges are shown in Figure 5. The SF sponge showed stripe-type porous morphology. Alginate showed a zigzag-type porous morphology. Silk fibroin and alginate blend sponges are macrophase separation mode.

### Differential scanning calorimetry

Thermal behavior measured by DSC is closely related to the structural characteristics of SF blend sponges. Figure 6 shows the DSC curves of SF/alginate blend sponges. The SF sponge showed an exothermic peak at around 125°C, attributed to the thermal crystallization of SF, and a strong endothermic peak at about 280°C, attributed to the thermal degradation of SF. On the other hand, alginate showed a strong characteristic exothermic peak at around 240°C that is attributed to the disintegration of the molecular side chains and main chains.<sup>14</sup> With increasing SF content, the characteristic exotherm, originated from alginate, became broader and shifted to a higher temperature than that of alginate itself. However, with increasing SA content, the endothermic peak of SF degradation was much broader than that of SF itself. Moreover, the thermal crystallization temperature of SF decreased and finally disappeared.

The thermal decomposition temperature of silk fiber is about 350°C, which is detected in the case of well-oriented fiber containing  $\beta$ -sheet structure.<sup>18</sup> Native and regenerated silk fibroin exhibited a crystallization exothermic peak at around 200°C and a main degradation endothermic peak at about 280°C.<sup>13,19,20</sup> According to our result [Fig. 6(a)], the thermal crystallization temperature of SF sponges was much lower than that of SF films. Thermal crystallization induced by heat is related to the rearrangement of SF molecular chain segments. The reason that the thermal crystallization temperature of SF sponges is lower than that of SF films is not clear but it can be explained that the rearrangement of molecular chain in SF sponges is easier than that in SF films. These phenomena are also expected to relate to the molecular density of SF sponges, which is lower than that of SF films. Moreover, the exothermic peak of SF/SA blend sponges decreased with increasing SA content. These results indicate that the crystallization of SF induced by heat was limited by incorporation of SA. FTIR spectroscopy showed that the conformation of SF was not changed by the incorporation of SA. SEM showed that the two polymers macrophase separated. Comparing these results, the molecular chains of SF sponges are restricted by the rigid polysaccharide chains of SA. Therefore, we conclude that, although the conformation of SF blend sponges are random coil structure, heat treatment did not affect the structural transition of SF in blend sponges.

### CONCLUSIONS

Silk fibroin/sodium alginate blend sponges were prepared and structural and physical properties were examined with various blend ratios. The structural and physical properties of SF blend sponges were investigated using FTIR, DSC, XRD, and SEM. Instrumental analysis showed that the conformation of silk fibroin in silk fibroin blend sponges was not influenced by blending with sodium alginate. On the other hand, DSC showed that the thermal crystallization of silk fibroin was interrupted by incorporation of sodium alginate. The structural characteristics of silk fibroin in blend sponges were not affected by blending with sodium alginate. However, the mechanical properties of silk fibroin blend sponges increased by blending with a rigid polysaccharide, sodium alginate. Therefore, silk fibroin/alginate blend sponges could be used as wound dressings because of their good mechanical properties and biocompatibility.

The support of the Korea Science and Engineering Foundation (KOSEF) (grant no. R01-2002-000-00391-0) is gratefully acknowledged.

### References

1. Minoura, N.; Aiba, S.; Higuchi, M.; Gotoh, Y.; Tsukada, M.; Imai, Y. *Biochem Biophys Res Commun* 1995, 208, 511.
2. Chiarini, A.; Petrini, P.; Bozzini, S.; Pra, I. D.; Armato, U. *Biomaterials* 2003, 24, 789.
3. Miyari, S.; Sugiura, M.; Fukui, S.; *Agric Biol Chem* 1978, 42, 1661.
4. Zhang, Y. *Biotechnol Adv* 1998, 16, 961.
5. Hanawa, T.; Watanabe, A.; Tsuchiya, T.; Ikoma, R.; Hidaka, M.; Sugihara, M. *Chem Pharm Bull* 1995, 43, 284.
6. Yamaura, K.; Kuranuki, N.; Suzuki, M.; Tanigami, T.; Matsuzawa, S. *J Appl Polym Sci* 1990, 41, 2409.
7. Kweon, H. Y.; Ha, H. C.; Um, I. C.; Park, Y. H. *J Appl Polym Sci* 2001, 80, 928.
8. Liang, C. X.; Hirabayashi, K. *J Appl Polym Sci* 1992, 45, 1937.
9. Kikuchi, A.; Kawabuchi, M.; Watanabe, A.; Sugihara, M.; Sakurai, Y.; Okano, T. *J Controlled Release* 1999, 58, 21.
10. Lai, H. L.; Abu'Khalil, A.; Craig, D. Q. M. *Int J Pharm* 2003, 251, 175.
11. Häuselmann, H. J.; Mauda, K.; Hunziker, E. B.; Neidhart, M.; Mok, S. S.; Michel, B. A.; Thonar, E. *Am J Physiol Cell Physiol* 1996, 271, C742.
12. Thomas, A.; Harding, K. G.; Moore, K. *Biomaterials* 2000, 21, 1797.
13. Tsukada, M.; Gotoh, Y.; Nagura, M.; Minoura, N.; Kasai, N.; Freddi, G. *J Polym Sci Part B: Polym Phys* 1994, 32, 961.
14. Xiao, C.; Weng, L.; Zhang, L. *J Appl Polym Sci* 2002, 84, 2554.
15. Asakura, T.; Watanabe, Y.; Uchida, A.; Winagawa, H. *Macromolecules* 1984, 17, 1075.
16. Liang, C. X.; Hirabayashi, K. *Sen-I-Gakkaishi* 1990, 46, 535.
17. Freddi, G.; Romano, M.; Massafra, M. R.; Tsukada, M. *J Appl Polym Sci* 1995, 56, 1537.
18. Kweon, H. Y.; Park, Y. H. *Korean J Seric Sci* 1994, 36, 138.
19. Nam, J.; Park, Y. H. *J Appl Polym Sci* 2001, 81, 3008.
20. Magoshi, J.; Nakamura, S. *J Appl Polym Sci* 1975, 19, 1013.